Microchimica Acta (2020) 187:644
https://doi.org/10.1007/s00604-020-04626-8

ORIGINAL PAPER

Electrospun nitrocellulose membrane for immunochromatographic test strip with high sensitivity

Xue Wang[1] · Dong Yang[2] · Shun-Tian Jia[3] · Ling-Ling Zhao[3] · Tong-Tong Jia[2] · Chao-Hua Xue[1,3]

Received: 21 June 2020 / Accepted: 28 October 2020

Abstract

The main goal of this work is to develop an economical, portable, disposable, and reliable point of care paper biosensor based on visualization, which can be used to detect viruses, bacteria, and proteins. However, the sensitivity of immunochromatography test (ICT) strips based on nitrocellulose to target detection has always been a problem. Here, we use an electrospun nitrocellulose (ENC) fiber membrane instead of traditional nitrocellulose fiber membrane to construct ICT strips for early pregnancy detection. By proper selection of the diameter of the ENC fiber to adjust the pore size, porosity, and morphology of the membrane, ICT strips with low flow rate and high protein loading were obtained. Based on these properties, a convenient and sensitive method for the colorimetric determination of human chorionic gonadotropin was developed. Under the optimal conditions, the detection limit of ICT based on ENC membrane is 10 mIU mL^{-1} ($S/N = 3$), the linear detection range is 5–1000 mIU mL^{-1}, and the linear relationship is $Y = 0.0434\,X - 0.0136$ ($R^2 = 0.9802$). In addition, the test strip has good specificity and stability, and will not produce false-positive results.

Keywords Immunochromatography test · Electrospun nitrocellulose membrane · Human chorionic gonadotropin · Point-of-care diagnosis

Introduction

The immunochromatography test (ICT) technique based on the specific bio-recognition has been promising as point-of-care diagnostics to provide fast and simple measurement because it is low-cost, portable, robust, and user-friendly. Attributed to these advantages, ICT strips, a major product of this technology, have been used in a wide variety of applications [1–5], including medical and body health [6–10], virus and bacteria [11, 12], water resources [13, 14], and food safety [15, 16]. Most of the commercialized ICTs, such as ovulation test paper [17], pregnancy test paper [18, 19], and urine test strips [20] sold in hospitals and pharmacies, have a main membrane support of nitrocellulose (NC) membrane that is conventionally used for the specific reaction between antibody and antigen. In recent years, a number of researchers explored different ICTs by using modified NC membranes or replacing the conventional NC membrane with other supports [21–24]. In order to reduce the flow rate and increase the interaction rate between the targets and gold nanoparticles-antibody probes conjugates, Yew [25] electrospun polycaprolactone (PCL) on the NC membrane to form a hydrophobic coating. The PCL-coated NC resulted in the binding of more complexes to the capture probes, which increased the sensitivity of the test strip by approximately tenfold as compared to the unmodified one. In order to change the pore size, porosity, surface groups, and surface area of the paper substrate and then increase the adsorption ability of biomolecules on paper substrate, Tang [26] treated NC membrane with cellulose nanofibers (CNFs) by immersion of the membrane into 2% CNFs solution followed by incubation.

Supplementary Information The online version contains supplementary material available at https://doi.org/10.1007/s00604-020-04626-8.

✉ Dong Yang
yangdong@sust.edu.cn

✉ Chao-Hua Xue
xuechaohua@126.com

[1] College of Environmental Science and Engineering, Shaanxi University of Science and Technology, Xi'an 710021, China

[2] College of Chemistry and Chemical Engineering, Shaanxi University of Science and Technology, Xi'an 710021, China

[3] College of Bioresources Chemical and Materials Engineering, Shaanxi University of Science and Technology, Xi'an 710021, China

Published online: 06 November 2020

The CNFs treatment made the sensitivity of nucleic acid LFAs in *Staphylococcus aureus* testing achieve a 20-fold enhancement. Additionally, they integrated sponge shunt into LFA to decrease the fluid flow rate and thus to enhance its analytical sensitivity, achieving tenfold signal enhancement in nucleic acid testing of HBV by optimizing the thickness, length, and hydrophobicity of sponge [27]. For the sake of decreasing the cost of the microfluidic sensors for biomedical and environmental analysis [28], natural cotton thread was used as a support for transfer and mixed analyte samples for immunochromatographic analysis [29]. Mao and Du [30–32] respectively prepared ICT strip biosensor with cotton thread replacing commercial NC membrane, and successfully realized the quantitative detection of specific antigens. Reinholt [33] presented PLA-based electrospun nanofibers as new material and alternative to the standard cellulose based papers for use in paper-based assays such as LFAs, and achieved result comparable to the nitrocellulose control. These works provided the opportunity and showed the necessity to develop new materials as support with significant advantages over their traditional counterparts.

Herein, nitrocellulose was fabricated into the nanofibrous membrane by an electrospinning method. In the process of electrospinning, the porosity and specific surface area of the membrane can be increased, and the flow rate of ICT substrate can be reduced by adjusting electrospinning parameters. Besides, due to the good biocompatibility of the spinning materials, the excellent adsorption performance of the membrane materials to the bioprotein macromolecules is conducive to the detection of sensitivity, specificity, and stability. The adsorption properties of membrane materials were researched by using the Lowry method and fluorescent protein adsorption ENC membrane method. A sensitive colorimetric method for the determination of human chorionic gonadotropin (HCG) using electrospun nitrocellulose membrane (ENC) as support for sandwich ICT strips was developed (Scheme 1).

Experimental

Materials

Nitrocellulose (NC) was purchased from Xingping Baotashan Coating Co., Ltd. (Shaanxi, China). Acetone, N, N-dimethylacetamide (DMF), sodium azide, sodium borate, methanol, Tween-20, and polyethylene glycol 20,000 (PEG-20000) were obtained from Sinopharm Chemical Reagent Co., Ltd. (Shanghai, China). Filter paper, conjugate pad, sample pad, absorbent pad, PVC backing plate, β-hCG antibody, α-hCG antibody, standard HCG samples, goat anti-mouse IgG, commercial NC (CNC) membrane (Sartorius CN140), and bovine serum albumin (BSA) were obtained from Shanghai JieYi Biotechnology Co., Ltd. (Shanghai, China). BSA-FITC was purchased from Beijing InnoChem Science & Technology Co., Ltd. (Beijing, China). Luteinizing hormone (LH) and follicle-stimulating hormone (FSH) were purchased from Shanghai Sangon Biotech Co., Ltd. (Shanghai, China). Double-distilled water was used for all the work.

Preparation of ENC membranes via electrospinning

Certain amount of nitrocellulose was dissolved in a mixture solvent of acetone and DMF (5:2, v/v) and gently stirred at room temperature for 24 h to obtain an NC solution for electrospinning. The electrospinning was carried out at room temperature using an electric field of 18 kV with the feeding rate kept constant at 2 mL h^{-1} by a syringe pump. The electrospun NC (ENC) fibers were deposited on a filter paper stuck on the aluminum collector, forming ENC membranes. The ENC membrane was taken out after several hours of electrospinning and dried in a vacuum oven at less than 40 °C overnight.

Here, ENC membranes from NC solutions of 17.8% (w/v), 19% (w/v), 21% (w/v), 26% (w/v), 31% (w/v), and 36% (w/v) were prepared and accordingly named as NC17.8, NC19, NC21, NC26, NC31, and NC36.

Morphology observation of NC membranes

Scanning electron microscope (SEM) images were obtained by a Hitachi S-4800 field emission scanning electron microscope. The samples were sputter-coated with gold prior to examination.

Performance testing of the NC membranes

Diffusion rate measurement of the NC membranes

The ENC membrane (4 cm × 0.5 cm) was immersed vertically into a microplate containing 60 μL AuNPs solution. The time required for the solution to flow through the entire membrane length was recorded. Each experiment was repeated three times, and the contrast experiment of the CNC membrane was carried out. According to the flow time of the liquid, suitable membrane was chosen as the substrate for strip assembly.

Evaluation of protein capacity and distribution on the membrane

The Lowry method was explored to quantitatively determine the amount of protein absorbed on the NC membranes. In a

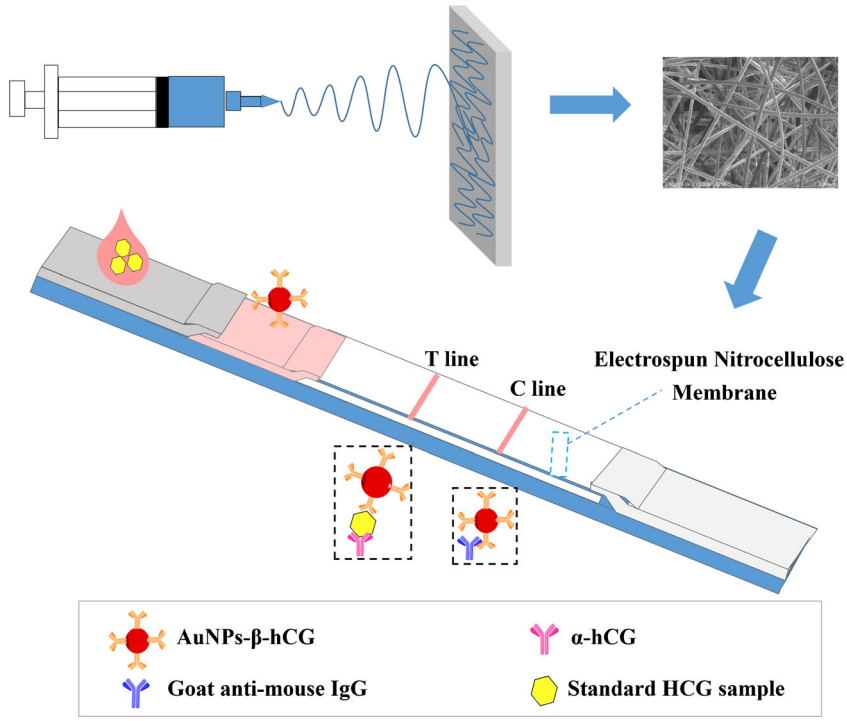

Scheme 1 Schematic of the preparation of ENC membranes by using the electrospinning method and the colorimetric determination of HCG on ICT test strips based on ENC membranes

typical experiment, a standard curve of BSA from 0 to 100 μg mL^{-1} was obtained, the absorbance was measured at 750 nm on a UV-vis spectrophotometer (Cary 5000, Germany). All experiments were repeated three times. Quantitative tests of protein capacity were performed by measuring the absorption rate of protein adsorbed on the membranes by a UV-Vis spectrophotometer using the formula (Eq. 1).

$$\text{Adsorption rate}(\%) = \frac{\overline{A}_0 - \overline{A}}{\overline{A}_0} \times 100\% \quad (1)$$

where $\overline{A}_0$ is the absorption of BSA solution with a concentration of 100 μg mL^{-1}, $\overline{A}$ is the absorption of the BSA solution after membrane adsorption.

FITC-BSA was used to observe the distribution of protein on the surface of the membranes. In a typical experiment, 100 μL of FITC-BSA solution was mixed with ENC membrane (1 cm × 1 cm) in a centrifuge tube and incubated in a shaker at 37 °C. After reaction for 1 h, the supernatant was removed, and then 4 mL distilled water was added to each centrifuge tube and washed at 37 °C for 1 h. Finally, the membranes were dried at room temperature and measured by confocal laser scanning microscopy (CLSM, LSM800, Carl Zeiss, Germany) to obtain the distribution of fluorescent proteins on the membrane surface. The average fluorescence intensity was calculated by Image J software, and the semi-quantitative results of average fluorescence intensity were obtained.

Preparation and assembly of lateral flow immunoassay strips

The sample pad, conjugate pad, ENC membrane, and absorbent pad were assembled in the PVC backing plate. Then α-hCG antibody and goat anti-rabbit IgG were separately spotted on the ENC membrane as the test line (T-line) and control line (C-line). The sample pad was saturated with 20 mM phosphate buffer (pH 7.4) containing 2.0% sucrose, 2.0% BSA, 0.1% sodium azide, and 20 mM sodium borate. The conjugate pad was saturated with 20 mM phosphate buffer (pH 7.4) containing 1.0% BSA. The ENC membrane was pretreated with phosphate buffer (pH 7.4) containing 3.0% BSA and 0.1% Tween-20. The strips were cut to 3.3 mm wide and stored in a zipper bag under room temperature drying conditions.

Assay procedure

The standard HCG samples of 10 IU mL^{-1} were diluted to different concentrations (5, 25, 50, 100, 500, and 1000 mIU mL^{-1}) with 20 mM PBS buffer solution (pH 7.4). Before each test, 10 μL Au-mAb complex was dropped on the binding pad, and then 100 μL HCG samples with different dilutions were dropped on the sample pad, and the detection results were observed after 15 min. When T-line and C-line are red, it is positive result; when only C-line is red, it is negative result. All experiments were repeated three times. At the same time, the optical density (OD) value of T line, which were analyzed by Image J software, was taken as the

ordinate, and the concentration of HCG sample was taken as abscissa to obtain a linear fitting line, and the lowest detection limit (LOD) was calculated. The LOD was defined as 3 times the blank/slope standard deviation ($S/N = 3$).

To verify the sensitivity of ICT strip, we tested the ICT strip with different concentrations of HCG sample (5, 25, 50, 100, 500, and 1000 mIU mL^{-1}, and negative control). The images were captured by mobile phone.

The specificity tests were performed by exploring antigens similar to HCG as targets, the antigens involved luteinizing hormone (LH) and follicle-stimulating hormone (FSH), and the concentrations of LH and FSH antigens were the same as HCG (100 mIU mL^{-1}).

Furthermore, in order to evaluate the feasibility of ENC membrane strip in the detection of real urine samples, HCG-positive urine and negative urine were used for analysis. In a typical experiment, we collected fresh urine from a pregnant woman as positive urine samples and that from a non-pregnant woman as negative urine samples. The positive urine samples were obtained by diluting the positive urine with ultrapure water into different concentrations (100%, 50%, 25%, 10%, 5%, 1%). The negative urine samples were used directly. One hundred microliters of the sample was added to the sample pad of the strip for test. The test results were observed after 15 min. Commercial pregnancy test strips were used for comparison.

Results and discussion

NC membranes morphology

SEM images of the ENC fibrous membranes with different concentrations of NC revealed a randomly oriented three-dimensional nonwoven structure (Fig. 1). As shown in Fig. 1a–f, ENC membranes exhibited structures with nanofibers.

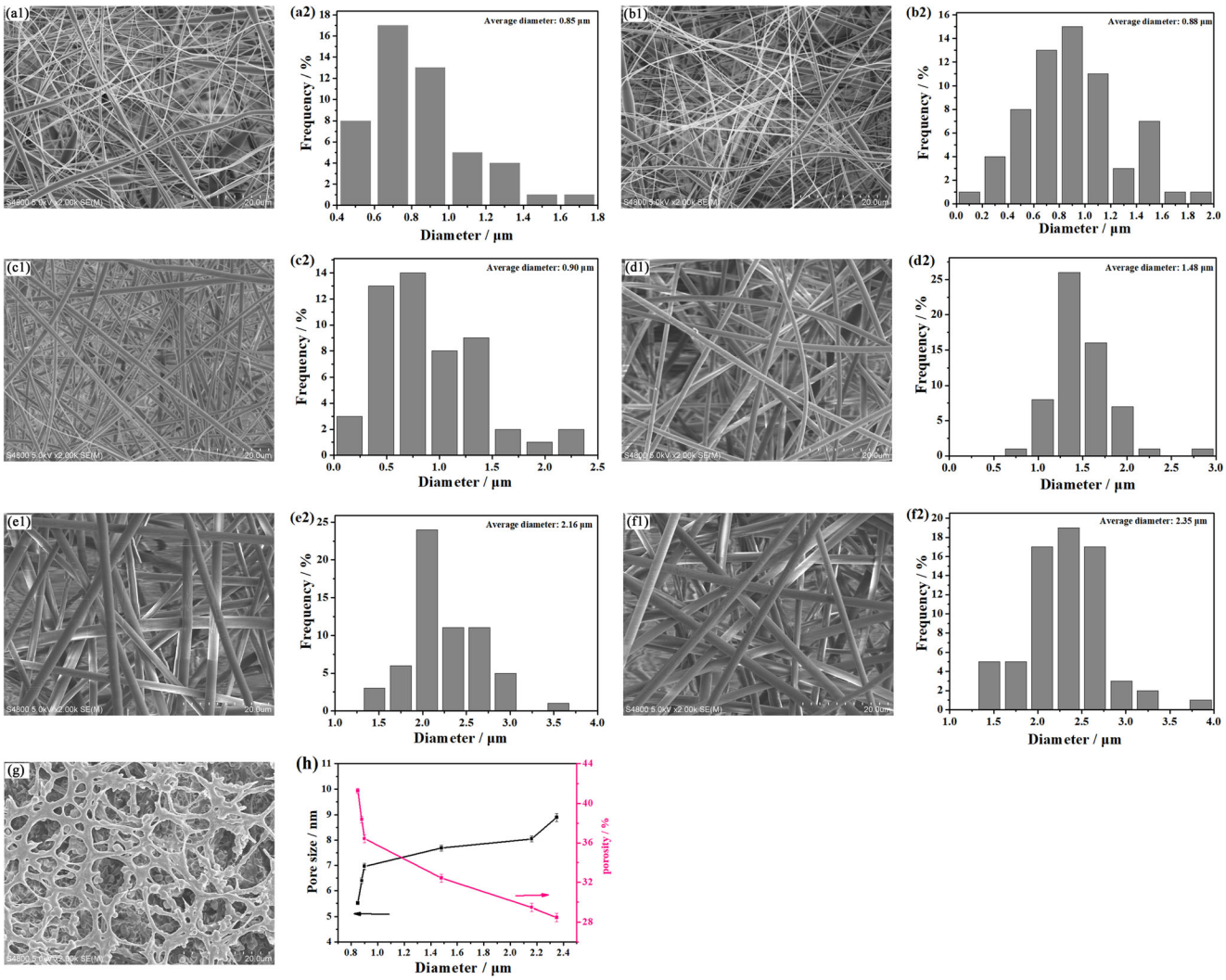

Fig. 1 SEM images and the corresponding diameter distribution of membranes of NC17.8 (**a**), NC19 (**b**), NC21 (**c**), NC26 (**d**), NC31 (**e**), and NC36 (**f**); SEM image of CNC membrane (**g**); the relationship between the diameter of the membrane fibers and the pore size and porosity, respectively (**h**)

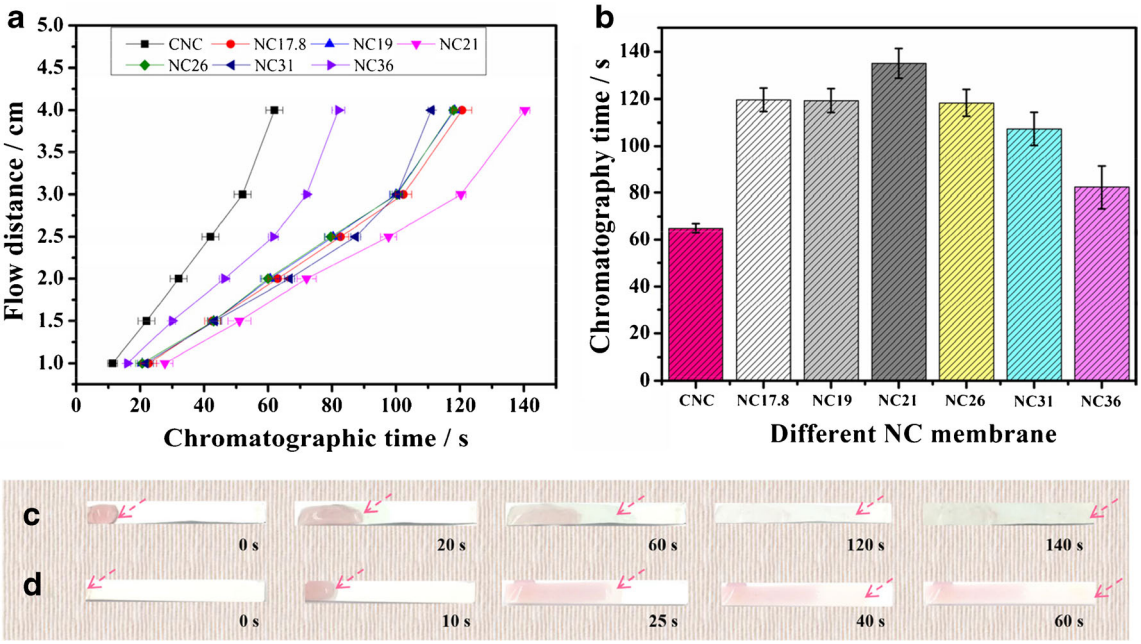

Fig. 2 The relationship between the chromatographic time of AuNPs solution on the surface of NC membrane and the flow distance (**a**); the flow time histogram of AuNPs solution on the surface of NC membranes (**b**); pictures of AuNPs solution chromatography on NC21 membrane (**c**), and CNC membrane at different times (**d**)

The NC17.8 and NC19 membranes showed a morphology with few elongated spindles and a large number of filamentous morphologies (average fiber diameter was 0.85 and 0.88 μm) were caused by the low NC solution viscosity and the insufficient stretching during the whipping of the jet in the electrospinning process.

When the concentration of the NC solution increased to 21%, 26%, 31%, and even 36%, the beads on the fibers were disappeared, and the corresponding average diameters of the fibers increased from 0.90 to 2.35 μm. When the mass fraction of the spinning solution is increased, the viscosity of the solution will also increase, and the ability to resist electric field-

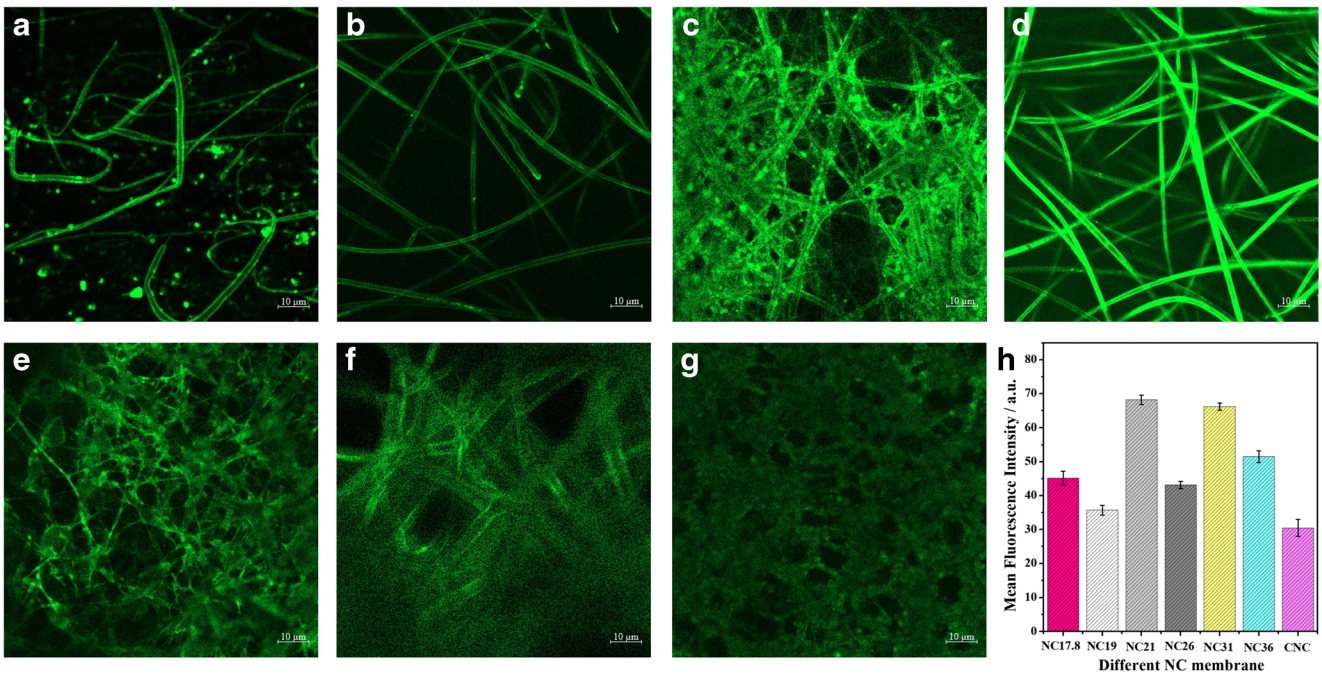

Fig. 3 Fluorescence microscopy images of NC17.8 (**a**), NC19 (**b**), NC21 (**c**), NC26 (**d**), NC31 (**e**), NC36 (**f**), and CNC (**g**); mean fluorescence intensity of membranes calculated by using Image J (**h**)

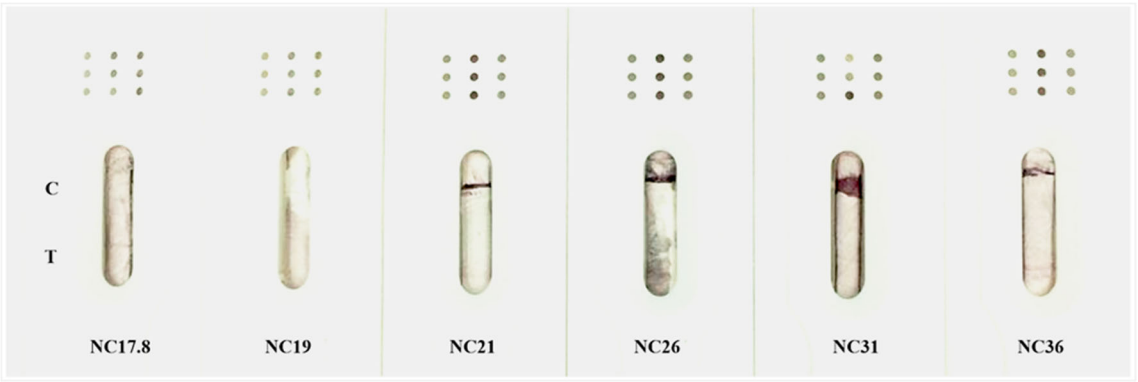

Fig. 4 Morphologies of C-line after an immune reaction on ICT strips based on different ENC membranes

stretching is enhanced. Therefore, when the applied voltage is constant, increasing the spinning solution concentration will increase the fiber diameter.

Figure 1g shows the morphology of the CNC membrane, which is network structure. Figure 1h expressed the relationship between the diameter of the membrane and the pore size and porosity, respectively. When the average fiber diameters of NC17.8, NC19, NC21, to NC36 membranes increased from 0.85 to 2.35 μm, the corresponding average fiber pore sizes increased from 5.5 ± 0.1 to 8.9 ± 0.17 nm, and the average fiber porosity decreased from 41.5 to 28.6%. The porosity of the membranes was dependent on the number of pores and decreased with the increasing NC concentrations.

Flow rate measurement of NC membrane

When we added the AuNPs solution on the surface of the NC membrane, the solution flows through the whole membrane. Figure 2a shows the position of liquid on the surface of the NC membrane at different times. When the solution flows through the half distance of the CNC membrane, it takes about 30 s. As the liquid slows down, time increases, the total time for the solution to flow through the membrane was nearly 60 s.

Figure 2b shows the flow rate of seven different NC membranes. It can be seen that the time of solution flowing through the CNC membrane is about 60 s, while the NC21 membrane is close to 140 s, and the time of other membranes all exceeded 80 s, which indicates the solution on the ENC membranes flow slower compared to CNC membrane.

Figure 2c and d show the comparison of the positions of NC21 and CNC membrane. The time of NC21 membrane needed in the same distance (4 cm) is longer, and the time of half and the entire distance was 60 s and 140 s respectively. By analyzing the morphology shown in Fig. 1, the NC21 membrane contains a large number of fibers with relatively low porosity and dense fiber accumulation, which requires more time for the solution to flow through. We assume that the flow rate is closely related to the morphology and structure of the membrane. This means that the fibrous membrane has a higher bulk density, and then produces a slower flow rate, which requires more flow time. As far as the flowing rate was concerned, the slower the liquid flowing through the membrane, the longer the bio-recognition occurs, and the more reactions of the antigen and the antibody would have. Therefore, ENC membranes with slower flowing rates are preferable for the assembly of ICT strips.

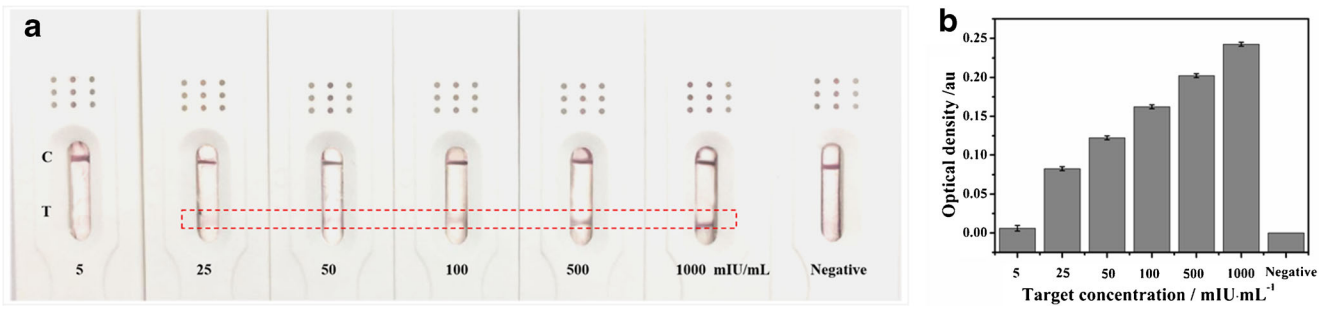

Fig. 5 The sensitivity test of ICT strips based on the NC21 membranes for different concentrations of HCG (**a**); OD value of the T-line in the ICT test strip (**b**)

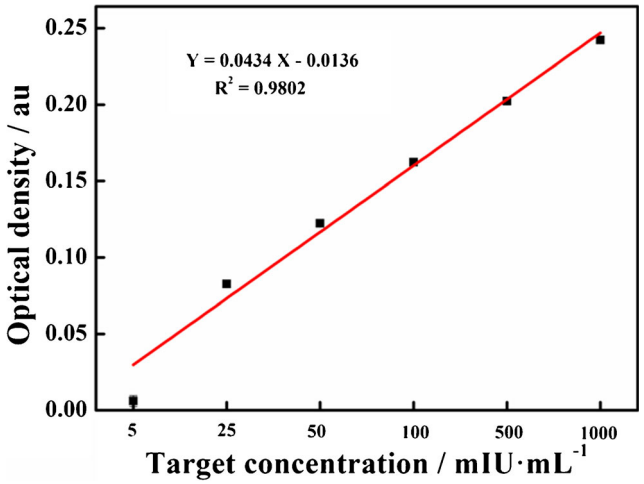

Fig. 6 Correlation between the concentration of HCG and its image optical density on T-line

The protein load capacity of NC membranes

FITC-BSA was used to qualitatively observe the protein absorption effect visibly on the surface of membranes, and then to test the fluorescence intensities by using laser confocal fluorescence microscopy. Figure 3a–g present the fluorescence microscopy images of ENC and CNC membranes, which show plenty of green fluorescence signals on the membranes. The fluorescence images of NC21 and NC31 show the brightest vision, and the fluorescence intensity was more than 60 a.u (Fig. 3h). Other membranes show pretty high intensities, exceeding 40 a.u, higher than the CNC membrane which is only closed to 35 a.u.

The Lowry method was used to quantitatively measure the protein load capacity of NC membranes utilizing the standard curve of BSA showing a downward trend linear relationship between protein content and absorbance (Fig. S1, Electronic Supporting Material). The standard equation was obtained to be $Y = 0.86159 + 0.0043\ X$ ($R^2 = 0.994$). According to the results of BSA protein adsorbed to NC membranes (Table S1, Electronic Supporting Material), the adsorption rate of ENC21 was calculated to be 17.02%, while the CNC was only 5.04%.

The results showed that the prepared ENC membranes have higher protein capacity and good protein adsorption performance, which provided great convenience for the immunoassay of ICT strip.

Optimization of the test strip

The results show that the intensities of C-line on the ENC membranes were different, as shown in Fig. 4. Red C-lines of NC21, NC26, NC31, and NC36 can be observed by naked-eyes, indicating the strips are valid. Taking the intensity and line shape of the C-line, and background color of the NC membranes into consideration, the line shape of NC36 and NC26 is incomplete, and the background color is obvious, which is not conducive to distinguish the effectiveness of bands.

The line shape of the NC36 and NC26 is not intact and the background color is obvious. The C-line of the NC31 strip is wider but the line shape is not regular; therefore, NC26, NC31, and NC36 strips are not suitable for assembling ICT strips. While the C-line of NC21 shows high intensity, no background color and regular shape. Taking the parameters of the flowing rate, protein capacity, the fluorescence intensity, and the test validity into consideration, the NC21 membrane was chosen as the most suitable membrane to develop ICT strips.

Test performance for HCG detection

Determination of the sensitivity of HCG

Figure 5a represents the sensitivity results of the test strip after HCG detection, and the minimum detection limit can be determined by observing the changes of optical signals on T-line and C-line. The T-line could not be seen when the

Table 1 An overview of recently reported nanomaterial-based optical methods for HCG

Materials used	Method applied	Specificity	LODs[3]	References
QD	LFAs	HCG	16	Li et al. 2018 [34]
AuNPs	LFA	HCG	2.8	Qu et al. 2020 [35]
CNTs	Electrochemical	HCG	5[4]	Viet et al., 2019 [36]
LS[1] nanophosphors	LFA	HCG	1[5]	Danthanarayana et al. 2019 [37]
Magnet	Novel immunoassay	HCG	0.19	Chen et al. 2019 [38]
MnO_2	Enzyme-catalyzed	HCG	0.36	Zhang et al. 2019 [39]
AuNFs[2]	ICAs	HCG	9	Zhang et al. 2019 [40]
Oligopeptide	Liquid crystals	HCG	1[6]	Ding et al. 2013 [41]
AuNPs	ICT	HCG	10	This work

[1] Luminescent; [2] gold nanospheres; [3] mIU/mL; [4] pg/mL; [5] ng/mL; [6] IU/mL

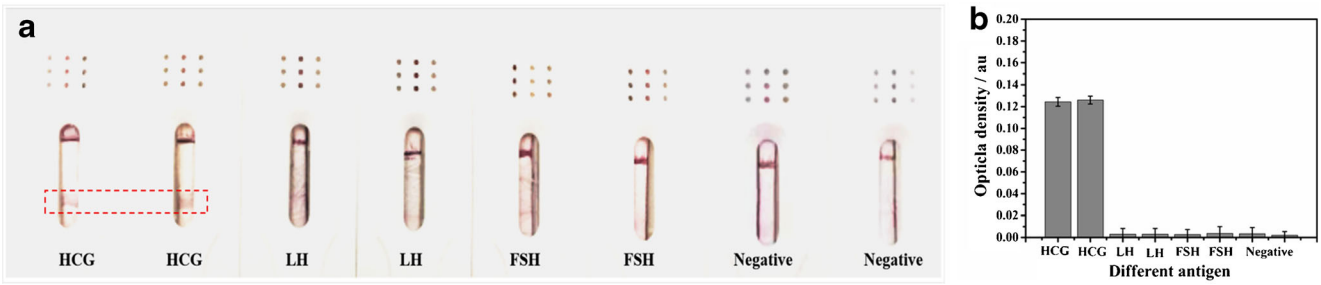

Fig. 7 The specificity test of ICT strips based on NC21 membrane for different antigens (**a**) and OD value of T-line in the ICT test strip (**b**)

concentration was 5 mIU mL^{-1}. With the increase of HCG concentration, the color of the T-line is gradually increased. When the concentration was 25 mIU mL^{-1}, a clear T-line could be seen by naked eyes on the strip. The results show that the NC21 membrane has the potential to develop an ICT strip for HCG detection.

To further examine the sensitivity of the strip, we tested the optical density (OD) of the T-line with different concentrations of HCG. As shown in Fig. 5b, when the concentration is 5 mIU mL^{-1}, there is almost no OD signal. However, as the concentration of HCG increased to 25 mIU mL^{-1}, the OD increased dramatically indication, and further increase of the HCG concentration increased the OD gradually, which means HCG can be detected at 25 mIU mL^{-1}. Such result makes the test strip possible to be used in real applications.

Real fresh urine sample test from a pregnant woman showed that the T-line of the NC21 strip showed clear positive result as that of the commercial pregnancy test strip (Fig. S2, Electronic Supporting Material). Although dilution of the urine made the color of the T-line of the NC21 strip gradually lighter, it showed positive results for a dilution of 5% urine sample, indicating the feasibility of the ENC membrane strip to detect real urine samples. However, further investigation of the ENC strip needs to be done to improve the sharpness and visibility of the T-line for positive detection.

Linear range and detection limit

Figure 6 shows that the proposed method exhibited independent linear correlations in the quantitative detection of HCG and the optical density value corresponding to the image increased with the concentration of HCG. The corresponding regression equations is expressed as followsq ($R^2 = 0.9802$). It can be seen that when the concentration of HCG is 5–1000 mIU mL^{-1}, the optical density of the image is linear with the concentration, and the LOD is 10 mIU mL^{-1}.

Table 1 shows an overview of the recently reported LOD values of the HCG optical method based on nanomaterials. The LOD of ENC-based strips for HCG is almost 2.5 times than that of commercially available pregnancy test strips (Table 1). A comparison of the recently reported methods for HCG detection with this research in Table 1 shows this method has advantages in fast detection, flexibility, high sensitivity, and versatility.

Specificity analysis

Besides sensitivity, the specificity evaluation of the strip is also an important parameter. Figure 7a shows the specificity result for HCG. It was found that no coloration occurred in the T-line, suggesting that no nonspecific binding existed and

Table 2 Comparison of the analytical results for HCG among different methods

Techniques	Modifiers	Advantage	Disadvantage	POC[3] or not	References
Immunosensor	ZnO	Intense PL[2]	Instrumental assistance	No	Rodrigues et al. 2020 [42]
Microfluidics immunoassay	Particle	Reduced reagent and time	Instrumental assistance	No	Piao et al. 2019 [43]
Photothermal immunoassay	PB[1]	Photothermal conversion	Instrumental assistance	No	Hong et al. 2019 [44]
Microfiber sensor	Fiber	Sensitive to temperature	Instrumental assistance	No	Chen et al. 2019 [45]
Aptasensor	GO	High-affinity material	Instrumental assistance	No	Chiu et al. 2019 [46]
Screen-printed sensor	Electrodes	Unique electrochemical behavior	Instrumental assistance	No	Samar et al. 2019 [47]
Liquid crystals	Oligopeptide	No antibody and label	Instrumental assistance	No	Ding et al. 2013 [41]
ICT	AuNPs	Controllable preparation of NC membrane	LOD needs to improve	Yes	This work

[1] Prussian blue; [2] Photoluminescence; [3] Point of care

thus the assay was indeed specific, indicating that utilizing the electrospun membrane is feasible to achieve high sensitivity of the strip. In order to further test the specificity, we detected the OD values of different T-lines (Fig. 7b). The results show that there is a significant difference between the OD value of the T-line of HCG, LH, and FSH. Only HCG has a strong OD signal, which indicates that the ICT strip has good specificity for the detection of HCG.

Besides, the advantages and disadvantages of using different methods to detect HCG are summarized in Table 2. It can be seen that different methods to detect HCG have their advantages, but the disadvantages are almost similar. When these novel methods or novel nanomaterials are used to detect HCG, it is necessary to have instrument assistance to obtain the results. Instrument assistance usually gets higher sensitivity, however, which is not immediate and real-time response. As for this method, the membrane is adjustable and controllable for the test strips; however, the LOD still needs to improve.

Conclusion

An ENC-based ICT strip has been successfully constructed realizing HCG detection with high sensitivity and specificity. By electrospinning, the membrane displays a higher specific surface area, lower flow rate, and higher protein loading capacity, which are helpful to overcome the defects of the traditional NC membrane. It is important to note that the availability of the ICT strip was improved by the electrospinning method, paving the way for the application of ENC in point-of-care testing fields. Based on this work, novel label nanomaterials could be integrated into ENC-based ICT strips to further increase the sensitivity to a greater extent. On the other hand, further work needs to be done to realize the sensitive and universal detection of other analytes in ENC-based ICT strips.

Funding This work was supported by Natural Science Foundation of Shaanxi Province (2020JM-506), National Natural Science Foundation of China (51572161), and major project of Ministry of Science and Technology of China (2017YFB0307700).

Compliance with ethical standards

Conflict of interest The authors declare that they have no competing interests.

References

1. Chen Y, Liu L, Cui G, Wu X, Kuang H, Xu C (2019) Development of an immunochromatographic strip for the detection of rosiglitazone in functional foods based on monoclonal antibodies. Anal Methods 11(38):4910–4916
2. Yu Q, Dou W, Liu J, Zhao G, Yang S, Zhu D, Zhao Y, Li L (2019) A sensitive and quantitative immunochromatographic assay for HBsAg based on novel red silica nanoparticles. Anal Methods 11(3):268–275
3. Hao K, Suryoprabowo S, Song S, Liu L, Kuang H (2017) Rapid detection of zearalenone and its metabolite in corn flour with the immunochromatographic test strip. Food Agric Immunol 29(1): 498–510
4. Kong MM, Yang B, Gong CJ, Wang H, LiX ZKS, Li JJ, Wu F, Liu X, Hu Z (2017) Development of immunochromatographic colloidal gold test strip for rapid detection of Haemophilus influenzae in clinical specimens. J Appl Microbiol 123(1):287–294
5. Zhang W, Duan H, Chen R, Ma T, Zeng L, Leng Y, Xiong Y (2019) Effect of different-sized gold nanoflowers on the detection performance of immunochromatographic assay for human chorionic gonadotropin detection. Talanta 194:604–610
6. Chen Y, Guo L, Liu L, Song S, Kuang H, Xu C (2017) Ultrasensitive immunochromatographic strip for fast screening of 27 sulfonamides in honey and pork liver samples based on a monoclonal antibody. J Agric Food Chem 65(37):8248–8255
7. Duan H, Huang X, Shao Y, Zheng L, Guo L, Xiong Y (2017) Size-dependent immunochromatographic assay with quantum dot nanobeads for sensitive and quantitative detection of Ochratoxin A in corn. Anal Chem 89(13):7062–7068
8. Ouyang H, Tu X, Fu Z, Wang W, Fu S, Zhu C, Du D, Lin Y (2018) Colorimetric and chemiluminescent dual-readout immunochromatographic assay for detection of pesticide residues utilizing g-C_3N_4/$BiFeO_3$ nanocomposites. Biosens Bioelectron 106:43–49
9. Pata S, Laopajon W, Pongpaiboon M, Thongkum W, Polpong N, Munkongdee T, Paiboonsukwong K, Fucharoen S, Tayapiwatana C, Kasinrerk W (2019) Impact of the detection of zeta-globin chains and hemoglobin Bart's using immunochromatographic strip tests for alpha(0)-thalassemia (-(SEA)) differential diagnosis. PLoS One 14(10):1–14
10. Wangman P, Chaivisuthangkura P, Taengchaiyaphum S, Pengsuk C, Sithigorngul P, Longyant S (2020) Development of a rapid immunochromatographic strip test for the detection of Vibrio parahaemolyticus toxin B that cause acute hepatopancreatic necrosis disease. J Fish Diseases 43(2):207–214
11. Li R, Meng C, Wen Y, Fu W, He P (2019) Fluorometric lateral flow immunoassay for simultaneous determination of three mycotoxins (aflatoxin B1, zearalenone and deoxynivalenol) using quantum dot microbeads. Microchim Acta 186(12):1–9
12. Kuijpers LMF, Chung P, Peeters M, Phoba MF, Kham C, Barbe B, Lunguya O, Jacobs J (2018) Diagnostic accuracy of antigen-based immunochromatographic rapid diagnostic tests for the detection of Salmonella in blood culture broth. PLoS One 13(3):1–16
13. Cinti S, Fiore L, Massoud R, Cortese C, Moscone D, Palleschi G, Arduini F (2018) Low-cost and reagent-free paper-based device to detect chloride ions in serum and sweat. Talanta 179:186–192
14. Song S, Zou S, Zhu J, Liu L, Kuang H (2017) Immunochromatographic paper sensor for ultrasensitive colorimetric detection of cadmium. Food Agric Immunol 29(1):3–13
15. Song S, Suryoprabowo S, Liu L, Zheng Q, Wu X, Kuang H (2019) Development of an immunochromatographic strip test for rapid detection of sodium nifurstyrenate in fish food. Agric Immunol 30(1):236–247
16. Liu B, Gong H, Wang Y, Zhang X, Li P, Qiu Y, Wang L, Hua X, Guo Y, Wang M, Liu F, Liu X, Zhang C (2018) A gold immunochromatographic assay for simultaneous detection of parathion and triazophos in agricultural products. Anal Methods 10(4): 422–428

17. Warsinke A (2009) Point-of-care testing of proteins. Anal Bioanal Chem 393(5):1393–1405
18. Tincello DG, Richmond DH (1998) Evaluation of reagent strips in detecting asymptomatic bacteriuria in early pregnancy: prospective case series. BMJ (Clinical research ed) 316(7129):435–437
19. Marino E, Threlfall WR, Schwarze RA (2009) Early conception factor lateral flow assays for pregnancy in the mare. Theriogenology 71(6):877–883
20. Hu J, Wang L, Li F, Han YL, Lin M, Lu TJ, Xu F (2013) Oligonucleotide-linked gold nanoparticle aggregates for enhanced sensitivity in lateral flow assays. Lab Chip 13(22):4352–4357
21. Jia X, Song T, Liu Y, Meng L, Mao X (2017) An immunochromatographic assay for carcinoembryonic antigen on cotton thread using a composite of carbon nanotubes and gold nanoparticles as reporters. Anal Chim Acta 969:57–62
22. Liu Y, Song T, Jia X, Meng L, Mao X (2017) Gold nanoparticles decorated carbon nanotube probe based immunochromatographic assay on cotton thread. Sens Actuat B-Chem 251:1112–1118
23. Meng LL, Song TT, Mao X (2017) Novel immunochromatographic assay on cotton thread based on carbon nanotubes reporter probe. Talanta 167:379–384
24. Zhou G, Mao X, Juncker D (2012) Immunochromatographic assay on thread. Anal Chem 84(18):7736–7743
25. Yew CT, Azari P, Choi JR, Li F, Pingguan-Murphy B (2018) Electrospin-coating of nitrocellulose membrane enhances sensitivity in nucleic acid-based lateral flow assay. Anal Chim Acta 1009: 81–88
26. Tang RH, Liu LN, Zhang SF, Li A, Li ZD (2019) Modification of a nitrocellulose membrane with cellulose nanofibers for enhanced sensitivity of lateral flow assays: application to the determination of Staphylococcus aureus. Microchim Acta 186(12):1–8
27. Tang R, Yang H, Gong Y, Liu Z, Li X, Wen T, Qu Z, Zhang S, Mei Q, Xu F (2017) Improved analytical sensitivity of lateral flow assay using sponge for HBV nucleic acid detection. Sci Rep 7(5):1–10
28. Nilghaz A, Ballerini DR, Shen W (2013) Exploration of microfluidic devices based on multi-filament threads and textiles: a review. Biomicrofluidics 11(15):1–16
29. Safavieh R, Zhou GZ, Juncker D (2011) Microfluidics made of yarns and knots: from fundamental properties to simple networks and operations. Lab Chip 11:2618–2624
30. Mao X, Du TE, Wang Y, Meng L (2015) Disposable dry-reagent cotton thread-based point-of-care diagnosis devices for protein and nucleic acid test. Biosens Bioelectron 65:390–396
31. Du TE, Wang Y, Zhang Y, Zhang T, Mao X (2015) A novel adenosine-based molecular beacon probe for room temperature nucleic acid rapid detection in cotton thread device. Anal Chim Acta 861:69–73
32. Mao X, Du TE, Meng LL, Song TT (2015) Novel gold nanoparticle trimer reporter probe combined with dry-reagent cotton thread immunoassay device for rapid human ferritin test. Anal Chim Acta 889:172–178
33. Reinholt SJ, Sonnenfeldt A, Naik A, Frey MW, Baeumner AJ (2014) Developing new materials for paper-based diagnostics using electrospun nanofibers. Anal Bioanal Chem 406(14):3297–3304
34. Li X, Gong X, Zhang B, Liu Y, Chang J, Zhang X (2018) Ultrasensitive lateral-flow assays based on quantum dot encapsulations with signal amplification. J Nanopart Res 20(5):139–153
35. Qu Z, Wang K, Alfranca G, Fuente JM, Cui D (2020) A plasmonic thermal sensing based portable device for lateral flow assay detection and quantification. Nanoscale Res Lett 15(1):10–22
36. Viet NX, Hoan NX, Takamura Y (2019) Development of highly sensitive electrochemical immunosensor based on single-walled carbon nanotube modified screen-printed carbon electrode. Mater Chem Phys 227:123–129
37. Danthanarayana AN, Finley E, Vu B, Kourentzi K, Willson RC, Brgoch J (2020) A multicolor multiplex lateral flow assay for high-sensitivity analyte detection using persistent luminescent nanophosphors. Anal Methods 12(3):272–280
38. Chen J, Hao L, Wu Y, Lin T, Li X, Leng Y, Huang X, Xiong Y (2019) Integrated magneto-fluorescence nanobeads for ultrasensitive glycoprotein detection using antibody coupled boronate-affinity recognition. Chem Commun 55(69):10312–10315
39. Zhang Z, Xu G, Xie L, Guan Y (2019) Colorimetric immunoassay for human chorionic gonadotropin by using peroxidase-mimicking MnO_2 nanorods immobilized in microplate wells. Microchim Acta 186(8):581–590
40. Zhang W, Duan H, Chen R, Ma T, Zeng L, Leng Y, Xiong Y (2019) Effect of different-sized gold nanoflowers on the detection performance of immunochromatographic assay for human chorionic gonadotropin detection. Talanta 194:604–610
41. Ding XK, Yang KL (2013) Antibody-free detection of human chorionic gonadotropin by use of liquid crystals. Anal Chem 85(22): 10710–10716
42. Rodrigues J, Pereira SO, Santos NF, Rodrigues C, Costa FM, Monteiro T (2020) Insights on luminescence quenching of ZnO tetrapods in the detection of hCG. Appl Surf Sci 527:146813–146823
43. Piao Y, Wang X, Xia H, Wang W (2018) Digital microfluidic platform for automated detection of human chorionic gonadotropin. Microfluid Nanofluid 23(1):1–8
44. Hong G, Zhang D, He Y, Yang Y, Chen P, Yang H, Zhou Z, Liu Y, Wang Y (2019) New photothermal immunoassay of human chorionic gonadotropin using Prussian blue nanoparticle-based photothermal conversion. Anal Bioanal Chem 411(26):6837–6845
45. Chen L, Liu B, Liu J, Wan SP, Wu T, Yuan J, Zhou X, Long K, Shao L, Fu YQ, He XD, Wu Q (2020) Novel microfiber sensor and its biosensing application for detection of hCG based on a singlemode-tapered hollow core-singlemode fiber structure. IEEE Sensors J 20(16):9071–9078
46. Chiu NF, Kuo CT, Chen CY (2019) High-affinity carboxyl-graphene oxide-based SPR aptasensor for the detection of hCG protein in clinical serum samples. Int J Nanomedicine 14:4833–4847
47. Damiati S, Haslam C, Sopstad S, Peacock M, Whitley T, Davey P, Awan SA (2019) Sensitivity comparison of macro- and micro-electrochemical biosensors for human chorionic gonadotropin (hCG) biomarker detection. IEEE Access 7:94048–94058